

Feedback controlled electromigration in four-terminal nano-junctions

ZhengMing Wu, M. Steinacher, R. Huber, M. Calame, S. J. van der Molen, and C. Schönenberger*
Institut für Physik, Universität Basel, Klingelbergstr. 82, CH-4056 Basel, Switzerland

We have developed a fast, yet highly reproducible method to fabricate metallic electrodes with nanometer separation using electromigration (EM). We employ four-terminal instead of two-terminal devices in combination with an analog feedback to maintain the voltage U over the junction constant. After the initialization phase ($U \lesssim 0.2$ V), during which the temperature T increases by $80 - 150$ °C, EM sets in shrinking the wire locally. This quickly leads to a transition from the diffusive to a quasi-ballistic regime (0.2 V $\lesssim U \lesssim 0.6$ V). At the end of this second regime, a gap forms ($U \gtrsim 0.6$ V). Remarkably, controlled electromigration is still possible in the quasi-ballistic regime.

PACS numbers: 81.07.Lk, 66.30.Qa, 73.63.Rt, 73.40.Jn, 73.23.Ad, 81.16.Nd

Single-molecule electronics has been the focus of substantial worldwide research [1]. Direct measurement of electron flow through a single molecule promises a better understanding of the electron transfer processes in molecules. To measure single molecules, small metallic junctions with nano-sized gaps are needed in between which molecules can then anchored and electrically measured.

Various methods have been developed to define and measure such molecular junctions [2]. Among these, electromigration (EM) induced nano-gaps have successfully been employed for a broad range of molecules, revealing various transport phenomena [3, 4, 5]. EM-junctions have the advantage that gates with a decent gate-to-molecule coupling can be fabricated [5]. However, the junction formation is a slow process and prone to instabilities. In addition, nano-particles can form during the EM-process through which electric transport may occur subsequently [6, 7, 8, 9]. Refined EM processes are therefore highly desirable. In this article we introduce a new technique that employs a fast analog electronic feedback to accurately control the voltage over the junction during the EM process.

Electromigration is the directed migration of atoms caused by a large electric current density. EM proceeds by momentum transfer from electrons to atoms and requires sufficient atom mobility to occur. The latter increases at higher temperatures, so that local Joule heating is an important parameter in addition to current density [10]. The formation of an EM nano-gap starts with the lithographic definition of a metallic wire with a constriction (junction), where the EM process will be effective. EM narrows the junction down, until a gap forms and the process self-terminates. In such lithographically defined wires, the bonding pads are far away from the constriction, yielding long leads with comparatively large lead resistances R_L . Typically, R_L is much larger than the resistance of the junction R_J (Fig. 1, inset). Although a voltage U_0 is applied, the junction is effectively current-biased through R_L . Consequently, as EM starts

shrinking the junction and R_J increases, the power dissipated on the junction grows proportional to R_J , which may cause a thermal run-away, destroying the junctions. This instability appears in the $I - U_0$ characteristics (see Fig. 1) along branch B, which is multi-valued. In the shaded region, the junction can rapidly be destroyed, if it switches, for example, at point **p** to the open state well above the breaking point **e**. Because this happens at much larger power dissipation than would be the case at point **e**, the junction is “burnt” off. In order not to destroy the junction, one therefore has to ensure that the process follows branch B. This can be done manually, or better by software control [11, 12]. This approach is however quite slow, as U_0 needs to be set back and slowly ramped up repetitively. It would be much better to remove the destructive region altogether. Point **s** occurs at larger U_0 values than point **e**, because $R_L \gg R_J$. Hence, designing devices with low lead resistances relaxes the problem [13]. We eliminate the lead resistances by defining *four* terminals to each junction and applying a novel and fast electronic feedback scheme.

The principle of our EM procedure is illustrated in Fig. 1b. The voltage drop over the junction U is controlled by a custom-made feedback voltage source. The four terminals are defined by two symmetric pairs of contacts, a left and a right pair (Fig. 1c-d). On one pair, the bias voltage U_0 is supplied, while on the other the voltage drop U over the junction is simultaneously measured. Regardless of the actual value of the junction resistance R_J , the feedback voltage source maintains U constant. This removes the thermal instability, because if $U = \text{const}$ while R_J evolves to larger values due to EM, the power over the junction decreases. A nano-gap is formed by ramping up $U_{ref} = U$ until the junction switches to a high-ohmic state with $R_J > 100$ k Ω at $U \simeq 0.4 \dots 0.6$ V. This is typically performed during a few minutes, but can be done faster [14] or slower with no observable difference. Because we would like to characterize the junction during the evolution of EM, we do not ramp U continuously but in a square-wave pattern. This is illustrated in Fig. 2c. We measure $R_J(U)$ at voltage U (arrows) and subsequently switch to $U \simeq 0$ to measure the instantaneous linear-response resistance of the junction $R_J^0(t)$

*Electronic address: christian.schoenenberger@unibas.ch

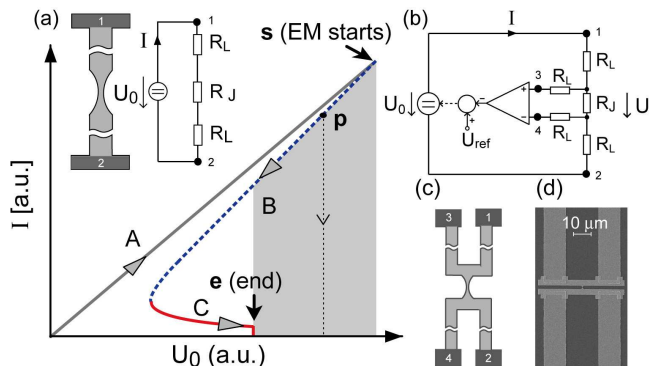


FIG. 1: Schematic characteristic of the current I versus bias voltage U_0 during software controlled 2-terminal electro-migration (EM) [11, 12]. EM starts at point s and the junction breaks open at point e . Insets: (a) schematics of the constriction forming the junction with attached leads and its equivalent circuit diagram. R_L , R_J are the lead and junction resistances, respectively. (b) The electric circuit for 4-terminal EM and (c) an SEM micrograph of an actual device. The voltage drop U over the junction is maintained constant and equal to a preset reference value U_{ref} by the feedback system.

with the aid of a small voltage modulation (lock-in technique). Although $R_J^0(t)$ is measured at $U \simeq 0$, we plot it as a function of U , enabling the comparison of $R_J(U)$ with R_J^0 . The whole process is performed at room temperature under ambient conditions.

Our devices are fabricated with two sequential lift-off processes on oxidized (400 nm) Si substrates using 50 nm Au together with a 5 nm thick Ti adhesion layer, where the latter is absent in the narrow junction region. The typical size of a fabricated Au constriction is 200 nm in length and 100 nm in width. The resistance of the junction R_J is around 3 – 10 Ω at room temperature whereas the overall resistance $R = R_J + 2R_L$ typically amounts to as much as 250 Ω .

Two representative graphs of the evolution of the junction resistance $R_J(U)$ (red) and the corresponding equilibrium resistance R_J^0 (black), measured while ramping up the junction voltage U , are shown in Fig. 2. Three regimes (I-III) can be discerned: in regime I, the constant equilibrium resistance R_J^0 shows that geometrically nothing happens. The sudden, but controlled increase in R_J (arrow) at $U = 0.15 \dots 0.2$ V signals the transition to regime II. Because R_J^0 has increased by typically one order of magnitude, the cross-section of the junction has consequently been decreased. R_J grows steadily with increasing junction voltage U , showing that EM is active. There is a second sudden jump occurring typically between $U = 0.4$ V and 0.6 V. In this transition to regime III, R_J grows from ≈ 1 k Ω to large values > 100 k Ω . Due to the large current drop, EM stops at this point leaving the junction ‘open’. In regime III, a gap has been formed and the device shows tunneling behavior. We in-

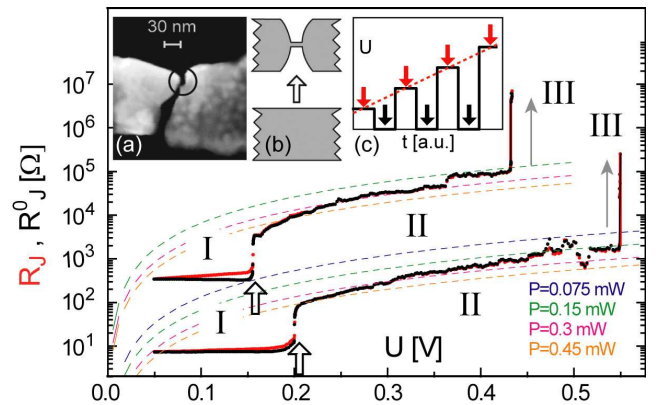


FIG. 2: Evolution of the junction resistance as function of junction voltage U during 4-terminal EM at room temperature for two devices. The upper curves are shifted by two orders of magnitude for clarity. The voltage U is ramped up in a square-wave pattern as illustrated in (c). After applying $U \neq 0$ during a short period and measuring the junction resistance $R_J(U)$ (red arrows), U is switched back to zero for a similar period of time during which the equilibrium resistance R_J^0 is measured (black arrows). A typical cycle lasts 0.1 s. The graph shows both $R_J(U)$ and R_J^0 during the whole process until the junction switches open into the tunneling regime with $R_J \gtrsim 100$ k Ω . The dashed curves are drawn as reference lines and correspond to constant power values, i.e. $P = U^2/R_J = const.$ P decreases from bottom (0.45 mW) to top (75 μ W). (a) an SEM micrograph of a typical junction after feedback EM and (b) an illustration of the slit formation after EM started.

deed measure non-linear $I(U)$ characteristics that follow the expected Simmons-law [15] quite well in this regime. Fig. 2a shows that EM tends to form slits that are typically smaller than 30 nm in width. Within these slits, there is a small part (indicated by a circle), which is even narrower. It is here that the gap is formed. More than 20 samples have been processed with this feedback method and in 18 of them, EM proceeded smoothly in the manner described before.

There are two remarkable features visible in Fig. 2. In the first place, R_J significantly differs from R_J^0 in regime I, whereas in regime II, R_J and R_J^0 are almost equal. In the second place, the transition from regime I to II, although appearing as a step, is gradual and rapidly flattens off again. Below, we argue that both these features point to a transition from the diffusive regime (regime I) to a ‘quasi-ballistic’ regime (regime II).

We first discuss regime I, which is diffusive given the size of our constriction. Upon increasing the voltage U , EM does not start immediately, as confirmed by a constant R_J^0 . As U increases further, the current density in the constriction increases. This leads to a higher local temperature, as witnessed by the increase of $R_J(U)$ with respect to R_J^0 . The temperature increase yields a strong rise in the atomic mobility [7, 12, 13, 16] and at a certain voltage, typically $U \lesssim 0.2$ V, EM becomes

considerable and the constriction starts to narrow down.

To estimate the local temperature close to the onset of EM, the difference between the junction resistances $R_J(U)$ and R_J^0 can be used [13, 17]. It can be related to a temperature difference ΔT alone if two conditions hold: i) the geometry does not change in between subsequent measurements of $R_J(U)$ and R_J^0 (small time delay); ii) the inelastic scattering length l_{in} is much smaller than the length of the junction L (diffusive regime). In this case, we may write $R_J(U) = R_J^0 \cdot (1 + \alpha \Delta T)$, where α is a constant which has to be measured independently. To do so, the resistivity ρ of a thin gold film with equal thickness was measured as a function of temperature T in the vicinity of $T = 25^\circ\text{C}$. $\rho(T)$ increases with T according to $(\rho(T) - \rho_0)/\rho_0 = 0.9 \cdot \Delta T$. Here, ρ_0 denotes the resistivity at $T = 25^\circ\text{C}$.

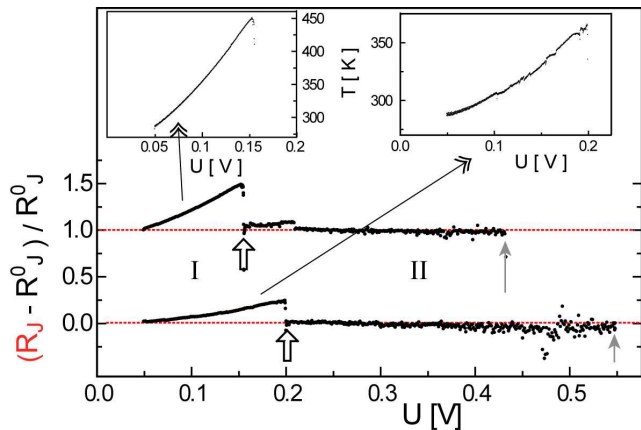


FIG. 3: The difference of the junction resistance $R(U)$ and $R_0(U=0)$. The two curves correspond to the same process as in Fig. 2. The up curve is shifted by 1 for clarity. In the insets are the development of local temperature in the junction before EM begins. The left inset is for the upper curve and the right inset for the lower curve. The procedure is carried out at room temperature.

In Fig. 3, we present $(R_J - R_J^0)/R_J^0$ as a function of the applied junction voltage U . The data correspond to the same two samples that gave rise to the measurements in Fig. 2. That R_J increases above R_J^0 in regime I, as we have emphasized before, can now be seen much clearer. The corresponding temperature increase is shown in the upper two insets. We see that ΔT reaches maximum values of 180°C and 90°C respectively, proving that a substantial temperature increase is required for EM to be initiated. This has been anticipated before [11, 12, 13] and is confirmed here.

Once regime II is entered, the difference between R_J and R_J^0 is surprisingly small. However, EM still takes place as evidenced by an increase in both R_J and R_J^0 . At first sight, this suggests that EM proceeds close to room temperature. While this conclusion is tempting, it rests on the assumption that the inelastic scattering length

l_{in} remains shorter than the effective junction length L in regime II as well. However, after entering regime II, the junction has narrowed and effectively shortened. In fact, SEM images such as the one in Fig. 2a indicate that the size of the slit is smaller than 30nm , a value close to the electron mean-free path [18]. This would then imply that a cross-over in the transport regime has taken place, from diffusive (‘viscous’ to be more precise) with $l_{in} \ll L$, to quasi-ballistic, with $l_{in} \simeq L$. We can then understand why our ‘thermometer’ ceases to work in regime II, because the resistance depends only slightly on temperature in the quasi-ballistic regime.

This picture becomes even more plausible, if we closely look at the data of Fig. 3 in regime II. The junction resistance $R_J(U)$ even slightly decreases compared to its equilibrium value R_J^0 as EM evolves, as if the temperature would decrease. This effect is very weak in the upper data set, but remarkably pronounced in the lower. It has been observed in the majority of electromigrated devices. This lowering can be understood if we assume that the current-voltage ($I-U$) characteristics becomes non-linear. This is the case when only a few scattering centers remain along the length of the junction. In the extreme case of a single scattering center (a tunnel barrier), $I(U)$ is not linear and increases stronger than linear above a characteristic energy scale, determining the strength of the scattering center. This again supports our conclusion that the effective junction length becomes shorter than the l_{in} in regime II, turning viscous electron motion into a quasi-ballistic one. This picture explains why the fast transition from regime I to regime II flattens off (see Fig. 2) and proceeds smoothly and well controlled down to the atomic scale. It does so because scattering is greatly reduced.

It may be considered surprising that EM proceeds at all in the quasi-ballistic regime. Although the number of scattering events decreases and slowing down EM in regime II, it implies that there is still enough scattering at the constriction to induce narrowing. To remove the last few atoms in the constriction, one needs to increase the bias by almost a factor of 3 to finally create a gap. During this process, the total dissipation is not constant, as conjectured by two groups [6, 11], but decreases (Fig. 2). To our knowledge, little work has been done on EM-induced narrowing of quasi-ballistic constrictions [19]. Understanding this paradoxical situation, will be advantageous for our full understanding of EM. This may prove beneficial for semiconductor industry, which uses thinner and thinner interconnects between devices.

This work has been supported by the Swiss National Center (NCCR) on “Nanoscale Science”, the Swiss National Science Foundation, and the European Science Foundation through the Eurocore program on Self-Organized Nanostructures (SONS). S.J.v.d.M. acknowledges The Netherlands Organization for Scientific Research, NWO (“Talent stipendium”).

-
- [1] for recent reviews, see: N. J. Tao, *Nature Nanotechnol.* **1**, 173 (2006); S. M. Lindsay and M. A. Ratner, *Adv. Mat.* **19**, 23 (2007).
- [2] for recent reviews, see: B. A. Mantooth and P. S. Weiss, *Proc. IEEE* **91**, 1785 (2003); D. K. James and J. M. Tour
- [3] H. Park, J. Park, A. K. L. Lim, E. H. Anderson, A. P. Alivisatos, and P. L. McEuen, *Nature*, **407**, 57 (2000).
- [4] J. Park, A. N. Pasupathy, J. I. Goldsmith, C. Chang, Y. Yaish, J. R. Petta, M. Rinkoski, J. P. Sethna, H. D. Abruna, P. L. McEuen, and D. C. Ralph, *Nature*, **417**, 722 (2002).
- [5] W. J. Liang, M. P. Shores, M. Bockrath, J. R. Long, and H. Park, *Nature*, **417**, 725 (2002).
- [6] A. A. Houck, J. Labaziewicz, E. K. Chan, J. A. Folk, and I. L. Chuang, *Nano Lett.*, **5**, 1685 (2005).
- [7] R. Sordan, K. Balasubramanian, M. Burghard, and K. Kern, *Appl. Phys. Lett.*, **87**, 013106 (2005).
- [8] H. B. Heersche, Z. de Groot, J. A. Folk, L. P. Kouwenhoven, and H. S. J. van der Zant, *Phys. Rev. Lett.*, **96**, 017205 (2006).
- [9] D. R. Strachan, D. E. Smith, M. D. Fischbein, D. E. Johnston, B. S. Guiton, M. Drndic, D. A. Bonnell, and A. T. Johnson, *Nano Lett.*, **6**, 441 (2006).
- [10] J. R. Black, *Proc. of IEEE* **57**, 1587 (1969).
- [11] D. R. Strachan, D. E. Smith, D. E. Johnston, T.-H. Park, M. J. Therien, D. A. Bonnell, and A.T. Johnson, *Appl. Phys. Lett.* **86**, 43109 (2005).
- [12] G. Esen and M. S. Fuhrer, *Appl. Phys Lett.* **87**, 263101 (2005).
- [13] M. L. Trouwborst, S. J. van der Molen, and B. J. van Wees, *J. Appl. Phys.* **99**, 114316 (2006).
- [14] The response time of this feedback system is better than $0.5 \mu\text{s}$.
- [15] J. G. Simmons, *J. Appl. Phys.* **34**, 1793 (1963).
- [16] M. F. Lambert, M. F. Goffman, J. P. Bourgoin, and P. Hesto, *Nanotechnology* **14**, 772 (2003).
- [17] B. Stahlmecke and Guenter Dumpich, *Defect and Diffusion Forum* **237-240**, 1163 (2005).
- [18] We estimate a mean-free path of 20 nm from the measured sheet resistance $R_{\square} \sim 1 \Omega$ of similar Au films using Drude's formula.
- [19] K. S. Ralls, D. C. Ralph and R. A. Buhrmann, *Phys. Rev. B* **40**, 11561 (1989); P. A. M. Holweg, J. Caro, A. H. Verbruggen, and S. Radelaar, *Phys. Rev. B* **45**, 9311 (1992).